

33 **ABSTRACT**

34 While the adult subependymal zone (SEZ) harbors pools of distinct neural stem cells that
35 generate different types of GABAergic interneurons, a small progenitor population in the
36 dorsal SEZ expresses *Neurog2* and gives rise to glutamatergic neurons. Here we investigated
37 whether SEZ progenitors can be programmed towards glutamatergic neurogenesis through
38 forced expression of *Neurog2*. Retrovirus-mediated expression of *Neurog2* induced the
39 glutamatergic neuron lineage markers *Tbr2* and *Tbr1* in cultured SEZ progenitors which
40 subsequently differentiated into functional glutamatergic neurons. Likewise, retrovirus-
41 mediated expression of *Neurog2* in dividing SEZ progenitors within the adult SEZ induced
42 *Tbr2* and *Tbr1* expression, hallmarking entry into the glutamatergic lineage also *in vivo*.
43 Intriguingly, *Neurog2*-expressing progenitors failed to enter the rostral migratory stream
44 (RMS) and instead differentiated directly within the SEZ or the adjacent striatum. In sharp
45 contrast, lentivirus-mediated postmitotic expression of *Neurog2* failed to reprogram early SEZ
46 neurons, which instead maintained their GABAergic identity and migrated along the RMS
47 towards the olfactory bulb. Thus, our data show that *Neurog2* can program SEZ progenitors
48 towards a glutamatergic identity, but fails to reprogram their postmitotic progeny.

49 INTRODUCTION

50 Accruing evidence indicates that neural stem cells (NSCs) lining the walls of the lateral ventricle
51 in the postnatal and adult subependymal zone (SEZ) exhibit regional identity thereby conferring
52 specific fate restrictions on NSCs (Azim et al., 2015; Lim and Alvarez-Buylla, 2014). Due to this
53 characteristic mosaic organization of the SEZ, NSCs residing in different SEZ domains along the
54 rostro-caudal and dorsal-ventral axes generate neurons of distinct subtype identities and become
55 subsequently destined for distinct sub-domains within the olfactory bulb (OB) (Brill et al., 2009;
56 Merkle et al., 2014; Merkle et al., 2007; Sequerra, 2014). Grafting experiments indicate that
57 these region-specific identities do not become erased upon placing NSCs into heterotopic
58 locations, arguing that extrinsic signals provided locally are not sufficient to reprogram the fate
59 restrictions of NSCs (Merkle et al., 2007). Furthermore, regional fate restrictions appear to
60 extend even to the decision between neuronal and glial fates as indicated by the fact that
61 oligodendroglial NSCs are enriched in the dorsal SEZ and *in vitro* clearly constitute a
62 lineage distinct from neurogenic NSCs (Ortega et al., 2013).

63 While the majority of NSCs from the adult SEZ give rise to several types of GABAergic or
64 tyrosine hydroxylase-expressing interneurons (Lim and Alvarez-Buylla, 2014), previous work
65 has shown that a small subpopulation of NSCs located in the dorsal SEZ can generate
66 juxtglomerular glutamatergic neurons (Brill et al., 2009). This subpopulation is characterized by
67 sequential expression of *Pax6*, *Neurog2*, *Tbr2*, and *Tbr1* (Brill et al., 2009) that characterizes
68 glutamatergic neuron producing lineages throughout the forebrain (Hevner et al., 2006). Forced
69 transcription factor expression can alter fate restrictions of neural cells beyond the stem cell
70 stage (Arlotta and Berninger, 2014). Forced expression of *Pax6* (Hack et al., 2005), *Dlx2* (Brill
71 et al., 2008), and *Fzf2* (Zuccotti et al., 2014) has been shown to shift subtype specification
72 within the adult SEZ *in vivo*. When cultured under neurosphere-conditions (high concentration of
73 epidermal growth factor (EGF) and fibroblast growth factor-2, (FGF2)), adult SEZ stem and
74 progenitor cells could be directed towards generation of fully functional glutamatergic neurons
75 by retrovirus-mediated expression of *Neurog2* (Berninger et al., 2007b). Moreover, upon
76 transplantation into the adult hippocampal dentate gyrus, *Neurog2*-expressing adult SEZ stem or
77 progenitor cells exhibited morphological similarities to endogenous dentate granule neurons and
78 some degree of functional integration (Chen et al., 2012). However, exposure to EGF and FGF2
79 exerts dramatic effects on NSCs that may include a partial loss of regional specification (Gabay
80 et al., 2003; Hack et al., 2004) and may render these cells more permissive to *Neurog2*. Thus, in
81 the present study we addressed the question whether *Neurog2* can overcome fate restrictions of
82 adult SEZ stem and progenitor cells in the absence of elevated growth factor signaling and drive

83 these towards acquisition of a glutamatergic phenotype, and if so, whether such effect extends
84 into the postmitotic life of adult-generated SEZ-derived neurons.

85

86

86 RESULTS

87 **Forced expression of *Neurog2* programs adult SEZ progenitors towards a glutamatergic** 88 **identity *in vitro***

89 Given that adult-generated glutamatergic OB neurons originate from progenitors located in the
90 dorsal part of the SEZ that express the proneural gene *Neurog2* (Brill et al., 2009) we wondered
91 whether ectopic expression of this transcription factor can program progenitors from the ventral
92 SEZ, which otherwise give rise exclusively to GABAergic neurons, towards a glutamatergic
93 neuron identity. To address this question we first took advantage of an adherent culture of the
94 adult SEZ (Costa et al., 2011; Ortega et al., 2011), which preserves the ratio of GABAergic and
95 glutamatergic neurogenesis as observed *in vivo* (Brill et al., 2009) and transduced proliferating
96 progenitors with a retrovirus encoding *Neurog2*, followed by the reporter *DsRed* behind an
97 internal ribosomal entry site (IRES; Fig. 1A). While cultures infected with a control virus
98 contained only very few neurons (identified by MAP2) expressing the vesicular glutamate
99 transporter-1 (vGluT1), forced expression of *Neurog2* resulted in a massive up-regulation of
100 vGluT1 (20-30 days post infection, DPI), localized to puncta presumably reflecting presynaptic
101 terminals (Fig. 1B). To confirm an actual glutamatergic re-specification, we directly assessed
102 whether *Neurog2*-expressing neurons exhibit glutamatergic synaptic transmission. To this end,
103 we performed pair recordings of neurons derived from *Neurog2*-expressing progenitors and non-
104 transduced control neurons 4 weeks after transduction (Fig. 1C). While synaptic transmission
105 mediated by control neurons was GABAergic in nature (Fig. 1C) as described previously (Costa
106 et al., 2011), stimulation of *Neurog2*-expressing cells in these pairs resulted in postsynaptic
107 currents that were fully blocked by the 2-amino-3-(3-hydroxy-5-methyl-isoxazol-4-yl)propanoic
108 acid (AMPA)/kainate receptor antagonist 6-cyano-7-nitroquinoxaline-2,3-dione (CNQX),
109 demonstrating its glutamatergic nature (Fig. 1C) (n= 6 pairs analyzed). This data demonstrates
110 that forced expression of *Neurog2* can program adult SEZ progenitors towards a glutamatergic
111 identity.

112

113 ***Neurog2*-mediated fate conversion of adult neural stem cell progeny *in vivo***

114 Next, we investigated the effects of forced *Neurog2* expression in the progeny of adult SEZ
115 NSCs *in vivo*. To this end, we stereotactically injected retroviruses encoding *DsRed* only, for
116 control, or *Neurog2*-IRES-*DsRed* as experimental manipulation into the adult SEZ. As expected,
117 after seven days, control virus infection revealed the characteristic picture of retrovirally labeled
118 cells migrating in chains along the entire extent of the rostral migratory stream (RMS) towards
119 the core of the olfactory bulb (OB) (Lois et al., 1996). Indeed, $44 \pm 7\%$ of cells were found in the

120 SVZ, $19 \pm 10\%$ of cells were migrating in the RMS and $37 \pm 9\%$ of cells reached the OB ($n= 3$
121 mice, 10197 cells analyzed, Fig. 2A-D and I). The DsRed-positive cells in the SEZ (Fig. 2B) and
122 the RMS (Fig. 2C) exhibited morphologies of migratory neuroblasts and upon reaching the OB
123 dispersed radially to establish themselves within the granular and glomerular layer (Fig. 2D). In
124 sharp contrast, progenitors expressing *Neurog2* exhibited a drastically altered migratory behavior
125 ($n= 3$ mice, 823 cells analyzed), abandoning chain migration ($1.5 \pm 1\%$ of cells in the RMS)
126 (Fig. 2E,G,I). As a consequence, only extremely few cells finally reached the OB ($2 \pm 2\%$) (Fig.
127 2E,H,I), while most of them remained in the SEZ area ($96 \pm 1\%$) (Fig. 2E,F,I). Moreover,
128 although the overall proportion of DCX-positive cells did not differ between control and
129 *Neurog2*-expressing cells (Fig. 3A,B and E-G), *Neurog2*-expressing neurons differentiated
130 within the SEZ or the adjacent striatum, with a highly complex dendritic arborization and high
131 density of dendritic spines (Fig. 3C,D) characteristic of projection neurons. None of these
132 morphologies were observed upon injection of the control virus. To further assess whether
133 *Neurog2*-transduced cells acquire a molecular glutamatergic neuron identity *in vivo*, we stained
134 for the T-box transcription factors Tbr2 and Tbr1, hallmarks of glutamatergic neurogenesis
135 (Hevner et al., 2006). Remarkably, Tbr2 was found to be expressed in $36 \pm 8\%$ of *Neurog2*-
136 expressing neurons ($n= 3$ mice, 7 DPI, 95 cells analyzed) located in the ventral SEZ, which
137 normally is devoid of cells expressing this transcription factor ($0.7 \pm 0.3\%$ of Tbr2-positive cells
138 among cells infected with the control retrovirus, $n= 3$ mice, 7 DPI, 962 cells analyzed) (Fig. 3H-
139 J). The acquisition of a glutamatergic neuron program by *Neurog2*-expressing cells was further
140 corroborated by the presence of a similar proportion of Tbr1-positive cells ($n= 2$, 7 DPI, 215
141 cells analyzed) (Fig. 3K).

142 143 **Forced expression of *Neurog2* in young postmitotic neurons does not result in** 144 **reprogramming towards a glutamatergic phenotype**

145 In the above experiments, use of retroviral vectors encoding *Neurog2* restricted transduction to
146 fast-dividing cells, most of which are transit-amplifying precursors (Costa et al., 2011; Doetsch
147 et al., 2002). We next asked whether conversion towards a glutamatergic identity would be
148 possible at later stages of lineage progression, i.e., after the last cell division when these cells
149 become postmitotic and commence differentiation.

150 Thus, we employed lentiviral vectors encoding *Neurog2* and *egfp* allowing for transduction of
151 non-dividing cells. In these constructs, expression of *Neurog2* and the reporter are driven by the
152 minimal human synapsin promoter (hSyn, Fig. 4A) restricting expression of *Neurog2* and *egfp* to
153 postmitotic neurons (Gascon et al., 2008). In fact, transduction of primary cortical cultures from

154 embryonic day E14 with the lentiviral vector hSyn-*Neurog2*-IRES-*egfp* resulted in efficient
155 expression of *Neurog2* and GFP proteins, which were both restricted to Tuj-1-immunoreactive
156 neurons (Fig. 4B). We then examined whether hSyn-driven expression of *Neurog2* in adult SEZ
157 cultures causes a similar conversion towards a glutamatergic identity as observed following
158 transduction at the precursor stage. In sharp contrast to the effect of *Neurog2* observed in
159 dividing progenitors, the vast majority of the lentivirus-transduced neurons remained
160 immunostaining-negative for vGluT1 at 30 days post infection (Fig. 4C), although vGluT1
161 positive neurons were readily detectable (Fig. 4D). However, their number did not differ from
162 cultures transduced with a control lentiviral vector (2.5% vs 4%, 701 cells analyzed) (Fig. 4E),
163 indicating that these few glutamatergic neurons represent the small endogenous glutamatergic
164 population derived from the dorsal portion of the adult SEZ (Brill et al., 2009). This data show
165 that forced *Neurog2* expression fails to convert immature postmitotic neurons derived from adult
166 NSCs into glutamatergic neurons *in vitro*.

167
168 ***Neurog2* activates the transcriptional program of glutamatergic neurogenesis in SEZ**
169 **progenitors, but fails to do so in young postmitotic neurons**

170 Forebrain glutamatergic neurogenesis is generally characterized by the sequential expression of
171 Tbr2 and Tbr1 (Hevner et al., 2006) and previous work has delineated the same expression
172 sequence in glutamatergic neurons derived from *Neurog2*-expressing SEZ progenitors (Brill et
173 al., 2009). Thus, we examined whether forced *Neurog2* expression results in the activation of the
174 same molecular pathway in adult SEZ progenitor cells. To this end, we transduced cultured SEZ
175 progenitors with the retrovirus encoding *Neurog2* and analyzed Tbr2 and Tbr1 expression at
176 days 7 and 9 post infection, respectively. Consistent with the natural program of glutamatergic
177 neurogenesis we observed expression of both transcription factors in *Neurog2*-expressing cells
178 (Fig. 5A,B). Tbr2 was expressed only in a subpopulation of *Neurog2*-transduced cells ($44 \pm 3\%$;
179 Fig. 5D), most likely due to the fact that this transcription factor is expressed transiently during
180 glutamatergic lineage progression (Hevner et al., 2006). We next transduced adult SEZ cultures
181 with the LV-hSyn-*Neurog2*-IRES-*egfp*. Contrary to the effect of retroviral expression at the
182 progenitor stage, expression of *Neurog2* in immature postmitotic neurons did not induce Tbr2
183 (Fig. 5A,D) or Tbr1 (data not shown) expression. This was more conspicuous as Tbr2 was found
184 to be expressed in a minor subpopulation of untransduced SEZ cells ($5 \pm 5\%$; Fig. 5A), again
185 reflecting the low degree of intrinsic glutamatergic neurogenesis from adult SEZ progenitors
186 (Brill et al., 2009). Finally, in agreement with the failure to activate a glutamatergic program,
187 neurons transduced with LV-hSyn-*Neurog2*-IRES-*egfp* maintained GABA immunoreactivity (94

188 $\pm 6\%$; Fig. 5C,D), while retrovirus-mediated *Neurog2* expression at the progenitor stage resulted
189 in a loss of GABA immunoreactivity in line with the acquisition of a glutamatergic phenotype
190 (Fig. 5C,D). Thus, this data not only confirm that *Neurog2*-transduced SEZ progenitors undergo
191 a fate conversion, but that this involves the recapitulation of glutamatergic neurogenesis from
192 adult SEZ progenitors under physiological conditions (Brill et al., 2009). On the other hand, the
193 failure of inducing a glutamatergic phenotype in young postmitotic neurons following forced
194 *Neurog2* expression is also accompanied by failure of inducing the stereotypical program of
195 glutamatergic lineage progression.

196
197 ***Neurog2* expression in young postmitotic neurons fails to induce a glutamatergic phenotype**
198 ***in vivo***

199 We next aimed to assess the effect of forced *Neurog2* expression in young postmitotic neurons
200 following stereotactic injection of LV-hSyn-*Neurog2*-IRES-*egfp* into the adult SEZ *in vivo* (Fig.
201 6). In contrast to the aberrant migration of cells transduced with a retrovirus encoding *Neurog2*
202 (Fig. 2), hSyn-driven *Neurog2* expression did not result in alterations in the migration program.
203 Indeed, DCX-positive cells were found to migrate normally via the RMS towards the OB
204 (control: $9 \pm 4.5\%$ of cells in SEZ, $3 \pm 0.6\%$ of cells in RMS and $88 \pm 5\%$ of cells in OB, n= 3
205 mice, 1929 cells analyzed; *Neurog2*: $10 \pm 4\%$ of cells in SEZ, $2.5 \pm 1\%$ of cells in RMS and $88 \pm$
206 5.5% of cells in OB, n= 3 mice, 855 cells analyzed; Fig. 6A). The presence of DCX-positive
207 cells expressing GFP while leaving the RMS indicates the early activity of the hSyn-promoter in
208 SEZ cells transduced with the LV-hSyn-*Neurog2*-IRES-*egfp* (Fig. 6B). Notably, at 10 DPI a
209 large number of transduced cells were already present in the OB and dispersed radially towards
210 the more superficial layers, where the majority acquired the morphology characteristic of
211 GABAergic granule or periglomerular neurons (Fig. 6C,D). Also at that late stage, we were
212 unable to detect expression of the glutamatergic lineage marker *Tbr2* in both, granule or
213 periglomerular neurons, amongst the LV-hSyn-*Neurog2*-IRES-*egfp* cells (Fig. 6E-F). This data
214 indicate that *Neurog2* expression at a postmitotic stage fails to reprogram the phenotype of
215 neurons derived from adult NSCs.

216

216 **DISCUSSION**

217 In the present study we demonstrate that forced expression of *Neurog2* redirects the program of
218 proliferating adult SEZ progenitors, mostly giving rise to GABAergic olfactory neurons, towards
219 generating neurons of the glutamatergic lineage. This indicates that *Neurog2* can override region
220 specific fate restrictions of adult NSCs. However, once SEZ-derived cells have differentiated
221 into postmitotic neurons, *Neurog2* can no longer induce a switch in transmitter phenotype, as
222 neurons retain their GABAergic neuron identity. Thus, there appears to be a restricted time
223 window during the lineage progression from stem cell to neuron during which *Neurog2* can alter
224 the program determining transmitter identity. Our data supporting a stage- and hence cellular
225 context-dependent potency of *Neurog2* are in line with a recent study showing that gain-of-
226 function of *Neurog2* can bias the balance between deep-layer and upper-layer neurogenesis
227 towards the former in early cortical progenitors, but has a limited capacity to specify early
228 neuronal features in late cortical progenitors (Dennis et al., 2017). Our data also provide
229 additional evidence for *Neurog2*'s instructive role for glutamatergic neurogenesis (Mattar et al.,
230 2008).

231 232 **Retroviral *Neurog2* expression directs dividing SEZ progenitors towards the glutamatergic 233 neuron lineage**

234 Retroviruses predominantly transduce fast-dividing progenitors both *in vitro* and *in vivo*. Thus,
235 by employing a retroviral vector for delivery of *Neurog2*, expression of the proneural gene
236 should be largely confined to activated stem cells and transit-amplifying progenitors as well as
237 dividing neuroblasts. We found that retrovirus-mediated *Neurog2* expression resulted in the
238 acquisition of a glutamatergic neuron identity *in vitro*, as evidenced by expression of the
239 glutamatergic lineage transcription factors *Tbr2* and *Tbr1* (Hevner et al., 2006), expression of
240 vesicular glutamate transporter and the development of glutamatergic synapses. In accordance
241 with a fate switch *in vivo*, *Neurog2*-expressing cells no longer migrated to the OB via the RMS,
242 but instead differentiated within the SEZ or the adjacent striatum. Of note, a recent study showed
243 SVZ cells can be redirected from their normal migration route and directed towards other brain
244 regions upon co-transduction with retroviruses encoding *Neurog2* and *Isl1* (Rogelius et al.,
245 2008). Thus, part of the fate switch induced by *Neurog2* is an alteration of the migratory
246 program normally under the influence of *Dlx2* (Brill et al., 2008). Besides this, differentiated
247 neurons derived from *Neurog2*-expressing progenitors developed morphological features
248 reminiscent of pyramidal-like neurons. Most importantly a substantial portion of the *Neurog2*-

249 expressing cells co-expressed Tbr2 and Tbr1, demonstrating entry into the glutamatergic neuron
250 lineage (Hevner et al., 2006).

251
252 ***Neurog2* fails to reprogram postmitotic neurons derived from SEZ progenitors towards the**
253 **glutamatergic neuron lineage**

254 In sharp contrast to the conspicuous effect of retrovirus-mediated *Neurog2* expression, targeting
255 *Neurog2* to postmitotic neurons by employing a lentivirus driving transgene expression from the
256 human synapsin promoter (Gascon et al., 2008) failed to alter the already ongoing program of
257 OB interneuron genesis. Lentivirally *Neurog2*-transduced cells continued to migrate along the
258 RMS to the OB where they took position within the granule cell layer for which most of the
259 adult-generated neurons in the SEZ are destined (Merkle et al., 2014; Merkle et al., 2007). Also,
260 in contrast to *Neurog2* expression in progenitors, postmitotic expression did not cause overt
261 changes in morphology and GFP-expressing cells exhibited morphologies highly reminiscent of
262 OB granule neurons. Moreover, primary cultures of neurons derived from SEZ progenitors were
263 GABA immunoreactive when *Neurog2* was expressed postmitotically. Finally, both *in vitro* and
264 *in vivo*, *Neurog2* failed to induce the expression of glutamatergic lineage transcription factors
265 such as Tbr2. In the absence of any evidence for a fate change, it thus appears that *Neurog2*-
266 expressing SEZ-derived neurons maintain the interneuron identity originally acquired during
267 lineage progression from stem cell to neuron. This data argues for the establishment of powerful
268 epigenetics barriers that impede a *Neurog2*-instructed switch from a GABA-to-glutamatergic
269 transmitter identity.

270
271 **Specific windows of opportunity for *Neurog2*-induced programming and reprogramming**

272 This data suggest that the potency of *Neurog2* sharply declines when neurons become
273 postmitotic and is likely linked to changes in the neuronal epigenome during this transition as
274 strongly indicated by the failure to upregulate Tbr2 which is known to be a direct target of
275 *Neurog2* (Kovach et al., 2013; Ochiai et al., 2009). Alternatively, or in addition to epigenetic
276 barriers, the effectiveness of *Neurog2* action may be curtailed by signaling mechanisms
277 regulating the phosphorylation state (Quan et al., 2016) or the formation of homo- versus
278 heterodimers (Li et al., 2012).

279 The failure of reprogramming at later stages of the stem cell to neuron lineage progression is
280 even more conspicuous given the capacity of *Neurog2* to sequentially induce Tbr2 and Tbr1
281 expression in astrocytes derived from the early postnatal cerebral cortex and reprogram these
282 into fully functional glutamatergic neurons (Berninger et al., 2007a; Heinrich et al., 2010). Yet,

283 also this reprogramming activity of proneural genes such as *Neurog2* or *Ascl1* appears to become
284 more restricted with glial maturation (Masserdotti et al., 2015; Ueki et al., 2015) and glia-to-
285 neuron conversion by *Neurog2* or *Ascl1* alone is very limited in the adult central nervous system
286 *in vivo* (Grande et al., 2013). Remarkably, some of these restrictions can be overcome by
287 allowing for enhanced epigenetic remodeling as recently demonstrated for *Ascl1*-induced
288 reprogramming of Müller glia into bipolar neurons in the lesioned adult mouse retina (Jorstad et
289 al., 2017). Moreover, a recent study identified a critical metabolic checkpoint for *Neurog2*- and
290 *Ascl1*-induced glia-to-neuron reprogramming which could be negotiated by co-expression of
291 *Bcl2* (Gascon et al., 2016). While this check point negotiation appears to work predominantly via
292 interference with reactive oxygen species-induced ferroptosis, it is conceivable that enhanced
293 reprogramming following *Bcl2* co-expression might also be related to the need of producing
294 larger quantities of particular mitochondrial metabolites required for epigenetic remodeling such
295 as shown in other systems (Wong et al., 2017).

296 The developmental window-specific actions of *Neurog2* on adult SEZ stem and progenitor cells
297 exhibit remarkable parallelism and differences to that of the transcription factor *Fezf2*. *Fezf2* was
298 originally described as a transcription factor to specify the fate of cortical progenitors towards a
299 corticofugal identity during development (Molyneaux et al., 2005). Subsequent work
300 demonstrated that it can reprogram striatal progenitors towards a corticofugal identity *in vivo*
301 (Rouaux and Arlotta, 2010) thus causing not only a similar transmitter identity switch (from
302 GABAergic to glutamatergic neuron) as described here for *Neurog2*, but also eliciting a specific
303 neuronal subtype conversion (from medium spiny neuron to corticofugal pyramidal neuron). Of
304 note, *Fezf2* reprogramming activity extends into early postmitotic life of a neuron but markedly
305 declines in the course of few days (Rouaux and Arlotta, 2013) arguing for the presence of a
306 critical window of nuclear plasticity that closes with epigenetic changes that occur during
307 neuronal maturation (Amamoto and Arlotta, 2014). More recently, *Fezf2* was found to program
308 NSCs in the postnatal and adult SEZ towards a glutamatergic neuron identity *in vitro* and *in vivo*
309 (Zuccotti et al., 2014). In conspicuous difference to the findings reported here for forced
310 *Neurog2* expression in fast-dividing cells, the *Fezf2*- induced fate switch was restricted
311 specifically to the stem cell stage and failed to convert both transit-amplifying progenitors or
312 dividing neuroblasts. Moreover, in contrast to the redirection of *Neurog2*-expressing neurons,
313 progeny of *Fezf2*-expressing NSCs still migrated to the OB. Thus, *Fezf2* and *Neurog2* appear to
314 possess distinct temporal windows of opportunity.

315 Taken together, our data provide evidence for remarkable plasticity within the lineage of adult
316 NSCs. It will be interesting to learn whether this plasticity can be harnessed towards translational

317 approaches to recruit adult NSC progeny into diseased brain tissue for repair (Benraiss et al.,
318 2013; Brill et al., 2009; Gage and Temple, 2013; Saghatelian et al., 2004). To fully exploit this,
319 it will be of crucial importance to identify the mechanisms underlying the closure of windows of
320 opportunity and thereby terminally sealing neuron fate.

321

321 MATERIAL AND METHODS

322 Ethical approval

323 All animal procedures were performed in accordance to the Policies on the Use of Animals and
324 Humans in Neuroscience Research, revised and approved by the Society of Neuroscience and the
325 state of Bavaria under license number 55.2-1-54-2531-144/07.

326

327 Plasmids and DNA constructs

328 Retroviral and lentiviral transduction of SEZ primary cultures was performed 2 hours after
329 plating the cells on glass coverslips, using VSV-G (vesicular stomatitis virus glycoprotein)
330 pseudotyped viruses. For the transduction with retrovirus we used the retroviral vectors RV-
331 pCAG-*Neurog2*-IRES-*DsRed* and RV-pCAG-IRES-*DsRed* as described previously (Heinrich et
332 al., 2011). To obtain the lentiviral vector *Syn-DsRed-Syn-egfp* we re-cloned a fragment
333 containing the cDNA of *Neurog2* and the internal ribosomal entry site from the RV-pCAG-
334 *Neurog2*-IRES-*DsRed* into the lentiviral vector *hSyn-DsRed-Syn-egfp* (Gascon et al., 2008). In
335 this case, control experiments were performed with the lentiviral vector *hSyn-egfp* (Gascon et
336 al., 2008).

337

338 SEZ primary culture

339 Following a previously established protocol by (Costa et al., 2011; Ortega et al., 2011), SEZ
340 cultures were prepared from the lateral wall of the lateral ventricle of young adult (8 - 12 weeks)
341 C57/Bl6 mice (*Mus musculus*) (Costa et al., 2011; Ortega et al., 2011). Briefly, tissue was
342 dissociated in 0.7 mg/ml hyaluronic acid (Sigma-Aldrich) and 1.33 mg/ml trypsin (Sigma-
343 Aldrich) in Hanks' Balanced Salt Solution (HBSS; Invitrogen) with 2 mM glucose (Sigma-
344 Aldrich) at 37°C for 30 minutes. After this enzymatic treatment, an equal volume of an ice-cold
345 medium consisting of 4% bovine serum albumin (BSA; Sigma-Aldrich) in Earle's Balanced Salt
346 Solution (EBSS; Invitrogen) buffered with 20 mM HEPES (Invitrogen) was added in order to
347 stop dissociation. Cells were then centrifuged at 200 *g* for 5 minutes, re-suspended in ice-cold
348 medium consisting of 0.9 M sucrose (Sigma-Aldrich) in 0.5× HBSS, and centrifuged for 10
349 minutes at 750 *g*. The cell pellet was re-suspended in 2 ml ice-cold medium consisting of 4%
350 BSA in EBSS buffered with 2 mM HEPES, and the cell suspension was placed on top of 12 ml
351 of the same medium and centrifuged for 7 minutes at 200 *g*. The resulting cell pellet was
352 resuspended in DMEM/F12 Glutamax (Invitrogen) supplemented with B27 (Invitrogen), 2 mM
353 glutamine (Sigma), 100 units/ml penicillin (Invitrogen), 100 µg/ml streptomycin (Invitrogen),
354 buffered with 8 mM HEPES. Finally, cells were plated on poly-d-lysine (Sigma) coated

355 coverslips at a density of 200-300 cells per mm² and, after 2 hours to allow for settlement of the
356 cells, cultures were treated with retroviral or lentiviral vectors for transduction.

357
358 **Viral vector injections**

359 Stereotactic injections of retrovirus and lentivirus were performed in 2 - 3 months old C57BL/6
360 male mice (*Mus musculus*). Prior to stereotactic injections, mice were anesthetized using
361 Ketamine (100 mg/kg; CP-Pharma) and Xylazine (5 mg/kg; Rompun; Bayer) and placed into a
362 stereotaxic frame. Approximately, 0.5 µl viral suspension was injected using a pulled-glass
363 capillary at the following coordinates relative to Bregma: 0.7 (antero-posterior), 1.2 (medio-
364 lateral) and 2.1-1.7 (dorso-ventral).

365
366 **Immunohistochemistry and immunocytochemistry**

367 Mice were deeply anesthetized using 5% chloralhydrate (wt/vol) diluted in phosphate buffered
368 saline and then perfused transcardially with saline (0.9%), followed by 4% paraformaldehyde
369 (PFA) (wt/vol) for 30 minutes. After this initial fixation, brains were dissected and post-fixed for
370 at least 2 hours in 4% PFA. Sagittal brain sections were prepared at a thickness of 50 µm using a
371 Thermo Scientific vibrating blade microtome.

372 For immunohistochemistry, sections were blocked for 90 minutes in TBS containing 0.3% Triton
373 and 5% donkey serum. Primary antibodies were diluted in blocking solution and incubated over
374 night at 4°C on the sections. In this study, we used antibodies to Tbr1 (Rabbit, 1:100 Abcam,
375 ab31940), Tbr2 (Rabbit, 1:500 Abcam, ab23345), RFP (Rabbit, 1:500 Rockland, 600401379S),
376 Doublecortin (DCX, Goat, 1:300 Santa Cruz Biotechnology, sc-8066) and GFP (Chicken,
377 1:1000, Aves labs, GFP-1020) The next day samples were washed with TBS and subsequently
378 incubated at room temperature for 1 hour with species-corresponding secondary antibodies made
379 in donkey and conjugated to Cy3 (1:500, Dianova, 711-165-152, 705-165-147), Alexa Fluor 488
380 (1:200, Invitrogen, A21206, A11055; Jackson Immunoresearch, 703-545-155) and Alexa Fluor
381 647 (1:500, Invitrogen, A31573, A21447). Sections were washed again in TBS, counterstained
382 with DAPI and mounted with an aqueous mounting medium.

383 Cultures were fixed in 4% PFA in PBS for 15 minutes at room temperature and processed for
384 antibody staining as described previously (Ortega et al., 2011).

385
386 **Electrophysiology**

387 Perforated patch-clamp recordings were performed as previously described (Heinrich et al.,
388 2011).

389

390 **Quantitative and statistical analysis**

391 Images stacks were acquired using a confocal microscope (Olympus FV1000 equipped with
392 x20/0.8 N.A., x40/1.35 and x60/1.42 N.A. oil-immersion objectives). Quantifications of marker-
393 positive cells were performed on single optical sections of an image stack. The percentage of
394 DCX-positive or Tbr2-positive cells was calculated among RFP-positive cells in the SEZ region.
395 For distribution analysis of the cells, RFP-positive/DCX-positive cells were quantified in the
396 SEZ, RMS and OB, and the percentage of cells in each region among total number of RFP-
397 positive/DCX-positive cells was calculated. The number of animals (n) used and the total
398 number of cells is indicated in the text. Data are represented as mean \pm s.d. Statistical analysis
399 was performed using SPSS Statistics 22 software. The statistical tests used and p values are
400 indicated in the figure legends.

401

402 **Acknowledgements**

403 We are grateful to Dr. Magdalena Götz for support throughout the project.

404

405 **Competing interests**

406 The authors declare no competing financial interests.

407

408 **Author contributions**

409 S.P., L.M.M and M.S.B designed and performed experiments, interpreted and analyzed results,
410 and wrote the manuscript. F.O. and M.K. designed and performed experiments. S.G.
411 conceptualized, designed and performed experiments, interpreted and analyzed results, and wrote
412 the manuscript. B.B. conceptualized the study and experiments, interpreted results, and wrote the
413 manuscript. All authors discussed the manuscript.

414

415 **Funding**

416 This work was supported by grants from the Deutsche Forschungsgemeinschaft (CRC1080,
417 INST 247/695-1), Belgian Science Policy Organization (Interuniversity attraction pole P7/20
418 "Wibrain") and ERA-NET NEURON (01EW1604) to B.B., and the Bavarian State Ministry of
419 Sciences, Research and the Arts consortium "ForIPS" to M.K. and B.B.

420

421 **References**

- 422 **Amamoto, R. and Arlotta, P.** (2014). Development-inspired reprogramming of the mammalian
423 central nervous system. *Science* **343**, 1239882.
- 424 **Arlotta, P. and Berninger, B.** (2014). Brains in metamorphosis: reprogramming cell identity within
425 the central nervous system. *Curr Opin Neurobiol* **27**, 208-214.
- 426 **Azim, K., Hurtado-Chong, A., Fischer, B., Kumar, N., Zweifel, S., Taylor, V. and Raineteau, O.** (2015).
427 Transcriptional Hallmarks of Heterogeneous Neural Stem Cell Niches of the Subventricular
428 Zone. *Stem Cells* **33**, 2232-2242.
- 429 **Benraiss, A., Toner, M. J., Xu, Q., Bruel-Jungerman, E., Rogers, E. H., Wang, F., Economides, A. N.,**
430 **Davidson, B. L., Kageyama, R., Nedergaard, M., et al.** (2013). Sustained mobilization of
431 endogenous neural progenitors delays disease progression in a transgenic model of
432 Huntington's disease. *Cell Stem Cell* **12**, 787-799.
- 433 **Berninger, B., Costa, M. R., Koch, U., Schroeder, T., Sutor, B., Grothe, B. and Gotz, M.** (2007a).
434 Functional properties of neurons derived from in vitro reprogrammed postnatal astroglia. *J*
435 *Neurosci* **27**, 8654-8664.
- 436 **Berninger, B., Guillemot, F. and Gotz, M.** (2007b). Directing neurotransmitter identity of neurones
437 derived from expanded adult neural stem cells. *Eur J Neurosci* **25**, 2581-2590.
- 438 **Brill, M. S., Ninkovic, J., Winpenny, E., Hodge, R. D., Ozen, I., Yang, R., Lepier, A., Gascon, S., Erdelyi,**
439 **F., Szabo, G., et al.** (2009). Adult generation of glutamatergic olfactory bulb interneurons.
440 *Nat Neurosci* **12**, 1524-1533.
- 441 **Brill, M. S., Snapyan, M., Wohlfrom, H., Ninkovic, J., Jawerka, M., Mastick, G. S., Ashery-Padan, R.,**
442 **Saghatelian, A., Berninger, B. and Gotz, M.** (2008). A *dlx2*- and *pax6*-dependent
443 transcriptional code for periglomerular neuron specification in the adult olfactory bulb. *J*
444 *Neurosci* **28**, 6439-6452.
- 445 **Chen, X., Lepier, A., Berninger, B., Tolkovsky, A. M. and Herbert, J.** (2012). Cultured subventricular
446 zone progenitor cells transduced with neurogenin-2 become mature glutamatergic neurons
447 and integrate into the dentate gyrus. *PLoS one* **7**, e31547.
- 448 **Costa, M. R., Ortega, F., Brill, M. S., Beckervordersandforth, R., Petrone, C., Schroeder, T., Gotz, M.**
449 **and Berninger, B.** (2011). Continuous live imaging of adult neural stem cell division and
450 lineage progression in vitro. *Development* **138**, 1057-1068.
- 451 **Dennis, D. J., Wilkinson, G., Li, S., Dixit, R., Adnani, L., Balakrishnan, A., Han, S., Kovach, C., Gruenig,**
452 **N., Kurrasch, D. M., et al.** (2017). Neurog2 and Ascl1 together regulate a postmitotic
453 derepression circuit to govern laminar fate specification in the murine neocortex. *Proc Natl*
454 *Acad Sci U S A* **114**, E4934-E4943.
- 455 **Doetsch, F., Petreanu, L., Caille, I., Garcia-Verdugo, J. M. and Alvarez-Buylla, A.** (2002). EGF converts
456 transit-amplifying neurogenic precursors in the adult brain into multipotent stem cells.
457 *Neuron* **36**, 1021-1034.
- 458 **Gabay, L., Lowell, S., Rubin, L. L. and Anderson, D. J.** (2003). Deregulation of dorsoventral patterning
459 by FGF confers trilineage differentiation capacity on CNS stem cells in vitro. *Neuron* **40**, 485-
460 499.
- 461 **Gage, F. H. and Temple, S.** (2013). Neural stem cells: generating and regenerating the brain. *Neuron*
462 **80**, 588-601.
- 463 **Gascon, S., Murenu, E., Masserdotti, G., Ortega, F., Russo, G. L., Petrik, D., Deshpande, A., Heinrich,**
464 **C., Karow, M., Robertson, S. P., et al.** (2016). Identification and Successful Negotiation of a
465 Metabolic Checkpoint in Direct Neuronal Reprogramming. *Cell Stem Cell* **18**, 396-409.
- 466 **Gascon, S., Paez-Gomez, J. A., Diaz-Guerra, M., Scheiffele, P. and Scholl, F. G.** (2008). Dual-promoter
467 lentiviral vectors for constitutive and regulated gene expression in neurons. *J Neurosci*
468 *Methods* **168**, 104-112.
- 469 **Grande, A., Sumiyoshi, K., Lopez-Juarez, A., Howard, J., Sakthivel, B., Aronow, B., Campbell, K. and**
470 **Nakafuku, M.** (2013). Environmental impact on direct neuronal reprogramming in vivo in the
471 adult brain. *Nat Commun* **4**, 2373.

- 472 **Hack, M. A., Saghatelian, A., de Chevigny, A., Pfeifer, A., Ashery-Padan, R., Lledo, P. M. and Gotz,**
473 **M.** (2005). Neuronal fate determinants of adult olfactory bulb neurogenesis. *Nat Neurosci* **8**,
474 865-872.
- 475 **Hack, M. A., Sugimori, M., Lundberg, C., Nakafuku, M. and Gotz, M.** (2004). Regionalization and fate
476 specification in neurospheres: the role of Olig2 and Pax6. *Mol Cell Neurosci* **25**, 664-678.
- 477 **Heinrich, C., Blum, R., Gascon, S., Masserdotti, G., Tripathi, P., Sanchez, R., Tiedt, S., Schroeder, T.,**
478 **Gotz, M. and Berninger, B.** (2010). Directing astroglia from the cerebral cortex into subtype
479 specific functional neurons. *PLoS Biol* **8**, e1000373.
- 480 **Heinrich, C., Gascon, S., Masserdotti, G., Lepier, A., Sanchez, R., Simon-Ebert, T., Schroeder, T.,**
481 **Gotz, M. and Berninger, B.** (2011). Generation of subtype-specific neurons from postnatal
482 astroglia of the mouse cerebral cortex. *Nat Protoc* **6**, 214-228.
- 483 **Hevner, R. F., Hodge, R. D., Daza, R. A. and Englund, C.** (2006). Transcription factors in glutamatergic
484 neurogenesis: conserved programs in neocortex, cerebellum, and adult hippocampus.
485 *Neurosci Res* **55**, 223-233.
- 486 **Jorstad, N. L., Wilken, M. S., Grimes, W. N., Wohl, S. G., VandenBosch, L. S., Yoshimatsu, T., Wong,**
487 **R. O., Rieke, F. and Reh, T. A.** (2017). Stimulation of functional neuronal regeneration from
488 Muller glia in adult mice. *Nature*.
- 489 **Kovach, C., Dixit, R., Li, S., Mattar, P., Wilkinson, G., Elsen, G. E., Kurrasch, D. M., Hevner, R. F. and**
490 **Schuermans, C.** (2013). Neurog2 simultaneously activates and represses alternative gene
491 expression programs in the developing neocortex. *Cereb Cortex* **23**, 1884-1900.
- 492 **Li, S., Mattar, P., Zinyk, D., Singh, K., Chaturvedi, C. P., Kovach, C., Dixit, R., Kurrasch, D. M., Ma, Y.**
493 **C., Chan, J. A., et al.** (2012). GSK3 temporally regulates neurogenin 2 proneural activity in the
494 neocortex. *J Neurosci* **32**, 7791-7805.
- 495 **Lim, D. A. and Alvarez-Buylla, A.** (2014). Adult neural stem cells stake their ground. *Trends Neurosci*
496 **37**, 563-571.
- 497 **Lois, C., Garcia-Verdugo, J. M. and Alvarez-Buylla, A.** (1996). Chain migration of neuronal precursors.
498 *Science* **271**, 978-981.
- 499 **Masserdotti, G., Gillotin, S., Sutor, B., Drechsel, D., Irmeler, M., Jorgensen, H. F., Sass, S., Theis, F. J.,**
500 **Beckers, J., Berninger, B., et al.** (2015). Transcriptional Mechanisms of Proneural Factors and
501 REST in Regulating Neuronal Reprogramming of Astrocytes. *Cell Stem Cell* **17**, 74-88.
- 502 **Mattar, P., Langevin, L. M., Markham, K., Klenin, N., Shivji, S., Zinyk, D. and Schuurmans, C.** (2008).
503 Basic helix-loop-helix transcription factors cooperate to specify a cortical projection neuron
504 identity. *Mol Cell Biol* **28**, 1456-1469.
- 505 **Merkle, F. T., Fuentealba, L. C., Sanders, T. A., Magno, L., Kessar, N. and Alvarez-Buylla, A.** (2014).
506 Adult neural stem cells in distinct microdomains generate previously unknown interneuron
507 types. *Nat Neurosci* **17**, 207-214.
- 508 **Merkle, F. T., Mirzadeh, Z. and Alvarez-Buylla, A.** (2007). Mosaic organization of neural stem cells in
509 the adult brain. *Science* **317**, 381-384.
- 510 **Molyneaux, B. J., Arlotta, P., Hirata, T., Hibi, M. and Macklis, J. D.** (2005). Fezl is required for the
511 birth and specification of corticospinal motor neurons. *Neuron* **47**, 817-831.
- 512 **Ochiai, W., Nakatani, S., Takahara, T., Kainuma, M., Masaoka, M., Minobe, S., Namihira, M.,**
513 **Nakashima, K., Sakakibara, A., Ogawa, M., et al.** (2009). Periventricular notch activation and
514 asymmetric Ngn2 and Tbr2 expression in pair-generated neocortical daughter cells. *Mol Cell*
515 *Neurosci* **40**, 225-233.
- 516 **Ortega, F., Costa, M. R., Simon-Ebert, T., Schroeder, T., Gotz, M. and Berninger, B.** (2011). Using an
517 adherent cell culture of the mouse subependymal zone to study the behavior of adult neural
518 stem cells on a single-cell level. *Nat Protoc* **6**, 1847-1859.
- 519 **Ortega, F., Gascon, S., Masserdotti, G., Deshpande, A., Simon, C., Fischer, J., Dimou, L., Chichung**
520 **Lie, D., Schroeder, T. and Berninger, B.** (2013). Oligodendroglial and neurogenic adult
521 subependymal zone neural stem cells constitute distinct lineages and exhibit differential
522 responsiveness to Wnt signalling. *Nat Cell Biol* **15**, 602-613.

- 523 **Quan, X. J., Yuan, L., Tiberi, L., Claeys, A., De Geest, N., Yan, J., van der Kant, R., Xie, W. R., Klisch, T.**
524 **J., Shymkowitz, J., et al.** (2016). Post-translational Control of the Temporal Dynamics of
525 Transcription Factor Activity Regulates Neurogenesis. *Cell* **164**, 460-475.
- 526 **Rogelius, N., Hebsgaard, J. B., Lundberg, C. and Parmar, M.** (2008). Reprogramming of neonatal SVZ
527 progenitors by islet-1 and neurogenin-2. *Mol Cell Neurosci* **38**, 453-459.
- 528 **Rouaux, C. and Arlotta, P.** (2010). Fezf2 directs the differentiation of corticofugal neurons from
529 striatal progenitors in vivo. *Nat Neurosci* **13**, 1345-1347.
- 530 ---- (2013). Direct lineage reprogramming of post-mitotic callosal neurons into corticofugal neurons in
531 vivo. *Nat Cell Biol* **15**, 214-221.
- 532 **Saghatelian, A., de Chevigny, A., Schachner, M. and Lledo, P. M.** (2004). Tenascin-R mediates
533 activity-dependent recruitment of neuroblasts in the adult mouse forebrain. *Nat Neurosci* **7**,
534 347-356.
- 535 **Sequerra, E. B.** (2014). Subventricular zone progenitors in time and space: generating neuronal
536 diversity. *Front Cell Neurosci* **8**, 434.
- 537 **Ueki, Y., Wilken, M. S., Cox, K. E., Chipman, L., Jorstad, N., Sternhagen, K., Simic, M., Ullom, K.,**
538 **Nakafuku, M. and Reh, T. A.** (2015). Transgenic expression of the proneural transcription
539 factor *Ascl1* in Muller glia stimulates retinal regeneration in young mice. *Proc Natl Acad Sci U*
540 *S A* **112**, 13717-13722.
- 541 **Wong, B. W., Wang, X., Zecchin, A., Thienpont, B., Cornelissen, I., Kalucka, J., Garcia-Caballero, M.,**
542 **Missiaen, R., Huang, H., Bruning, U., et al.** (2017). The role of fatty acid beta-oxidation in
543 lymphangiogenesis. *Nature* **542**, 49-54.
- 544 **Zuccotti, A., Le Magueresse, C., Chen, M., Neitz, A. and Monyer, H.** (2014). The transcription factor
545 *Fezf2* directs the differentiation of neural stem cells in the subventricular zone toward a
546 cortical phenotype. *Proc Natl Acad Sci U S A* **111**, 10726-10731.

547

548

548 **FIGURE LEGENDS**

549 **Figure 1. Retrovirus-mediated expression of *Neurog2* induces a glutamatergic phenotype in**
550 **adult SEZ progenitors. (A)**, Scheme of the retroviral vectors (RV) CAG-*Neurog2*-IRES-*DsRed*
551 and control CAG-IRES-*DsRed* used in this study. **(B)**, Immunocytochemistry of SEZ cultures 30
552 days after transduction with the RV CAG-*Neurog2*-IRES-*DsRed* or the corresponding control
553 RV CAG-IRES-*DsRed*. Note that *Neurog2*-expressing cells (right panel; red) are
554 immunopositive for vGluT (green) and MAP2 (blue), indicating a neuronal glutamatergic
555 phenotype. In contrast, cells infected with the *DsRed*-only-encoding vector (left panel; red)
556 remain negative for vGluT. **(C)**, Patch-clamp recording revealing the glutamatergic identity of
557 neurons derived from *Neurog2*-expressing SEZ progenitors. Micrographs show *Neurog2*-
558 expressing cells as indicated by the *DsRed* fluorescence (left panel) and the recording
559 configuration (right panel). The cell marked with the black asterisk expresses *Neurog2* (*DsRed*-
560 positive in the left panel), while the cell marked by the white asterisk is untransduced (*DsRed*-
561 negative in the left panel). Following step depolarisation of the untransduced cell a postsynaptic
562 response is elicited in the *Neurog2*-expressing cell that reversed at a membrane potential more
563 negative than -40 mV characteristic of GABAergic transmission and consistent with the
564 GABAergic nature of the untransduced neuron (left trace). In contrast, stimulation of the
565 *Neurog2*-expressing neuron resulted in a postsynaptic response that was abolished by the
566 AMPA/kainate receptor antagonist CNQX, demonstrating the glutamatergic neuron identity of
567 the *Neurog2*-expressing neuron (right trace). Scale bars: 10 μ m (B), 20 μ m (C).

568 **Figure 2. Retrovirus-mediated *Neurog2* expression *in vivo* alters the migration behaviour of**
569 **SEZ progenitors. (A-D)**, Sagittal view of an adult mouse brain depicting SEZ cells transduced
570 with the control RV CAG-IRES-*DsRed* (red) (B), migrating through the RMS (C) and reaching
571 the OB (D). **(E-H)**, Micrographs showing cells transduced with the RV CAG-*Neurog2*-IRES-
572 *DsRed* (red). At 7 DPI, only few transduced neuroblasts partially entered the RMS (G) and failed
573 to reach the core of the OB (H). They instead remained stationary in the anterior portion of the
574 SEZ (F). **(I)**, Quantification of the number of DCX-positive/*DsRed*-positive infected cells in the
575 SVZ, RMS and OB at 7 DPI. Error bars indicate mean \pm s.d., n=3/group. * $p < 0.05$, ** $p < 0.01$,
576 *** $p < 0.001$, One-Way ANOVA followed by Tukey's HSD post-hoc test. Scale bars: 1 mm
577 (A,E), 500 μ m (B-D and F-H).

578 **Figure 3. Retrovirus-mediated *Neurog2* expression induces a glutamatergic neuron identity**
579 ***in vivo*. (A,B)**, Micrographs depicting transduced SEZ cells with either control RV (red) (A) or
580 RV CAG-*Neurog2*-IRES-*DsRed* (red) (B) co-expressing DCX (green) at 7 DPI. Note that some

581 *Neurog2*-transduced neuroblasts invade the adjacent striatum. **(C,D)** Higher-power images
582 showing a *Neurog2*-transduced cell with neuronal morphology (C) and spines (D). **(E,F)**,
583 Micrographs depicting transduced cells immune-positive for DCX (green) **(G)**, Quantification of
584 the percentage of DCX-positive cells among infected cells. Error bars indicate mean \pm s.d., n.s.,
585 non-significant, t-test. **(H-I)**, Micrographs showing the expression of the transcription factor
586 Tbr2 (green) in SEZ cells forced to express *Neurog2* (I), while cells infected with the control
587 retrovirus lack Tbr2 expression (H). **(J)**, Quantification shows that more than one-third of
588 *Neurog2*-expressing cells up-regulated Tbr2. Error bars indicate mean \pm s.d., n=3/group.
589 $**p < 0.01$, t-test. **(K)**, Micrograph depicting Tbr1 expression (green) in cells transduced with the
590 RV CAG-*Neurog2*-IRES-*DsRed* (red). Scale bars: 100 μ m (A,B), 10 μ m (C), 5 μ m (D), 25 μ m
591 (E,F), 20 μ m (H,I,K).

592 **Figure 4. Forced *Neurog2* expression fails to induce a glutamatergic phenotype in**
593 **postmitotic neurons derived from SEZ progenitors. (A)**, Scheme of lentiviral vectors hSyn-
594 *Neurog2*-IRES-*egfp* and hSyn-*egfp* used. **(B)**, Micrographs show the expression of *Neurog2*
595 protein (red) and GFP (green) in primary cortical cultures from embryonic day E 14, 6 days after
596 transduction with the hSyn-*Neurog2*-IRES-*egfp* lentiviral vector (right panel), or the control
597 lentiviral vector encoding only GFP (left panel). Note that the human synapsin (hSyn) promoter
598 drives selective expression of the transgene in Tuj-1 neurons (blue). **(C)**, In adult SEZ primary
599 cultures, most of the neuroblasts transduced with the Syn-*Neurog2*-IRES-*gfp* do not differentiate
600 into vGluT-positive (red) glutamatergic neurons at 30 DPI. **(D,E)** Example micrographs of
601 *Neurog2*-expressing neurons (hSyn-*Neurog2*-IRES-*egfp*) (D) and control neurons (hSyn-*egfp*)
602 (E) exhibiting vGluT immunoreactivity, indicative of the rare presence of endogenous
603 glutamatergic neurons. Scale bars: 50 μ m (B-E).

604 **Figure 5. *Neurog2* induces hallmarks of the glutamatergic lineage when expressed in**
605 **dividing progenitors but not in young postmitotic neurons. (A)**, Cells from SEZ cultures
606 infected with the RV CAG-*Neurog2*-IRES-*DsRed* differentiate into Tuj-1-positive neurons
607 expressing the early glutamatergic transcription factor Tbr2 (right panel, arrows) at 7 DPI, while
608 those cells infected with the lentiviral hSyn-*egfp* control vector fail to express Tbr2 (left panel).
609 Note the cluster of non-transduced progenitors expressing Tbr2 (arrowheads) occurring at low
610 frequency in SEZ cultures. **(B)**, At later time points (9 DPI), neurons derived from progenitors
611 transduced with RV CAG-*Neurog2*-IRES-*DsRed* also express Tbr1 (arrows). **(C)**, Tuj-1-positive
612 SEZ neuroblasts transduced with RV CAG-*Neurog2*-IRES-*DsRed* are devoid of GABA
613 immunoreactivity at 7 DPI (right panel, arrowheads) while neuroblasts transduced with the

614 lentiviral vector Syn-*neurog2*-IRES-*egfp* remain immunoreactive for GABA (left panel, arrows).
615 **(D)**, Quantification of the proportions of transduced cells immunoreactive for Tbr2 or GABA at
616 7 DPI following retro- or lentiviral-mediated expression of *Neurog2*. Error bars indicate mean \pm
617 s.d. ** $p < 0.01$, *** $p < 0.001$, t test. Scale bars: 60 μm (A-C).

618 **Figure 6. Expression of *Neurog2* fails to induce a glutamatergic phenotype in postmitotic**
619 **neurons derived from SEZ progenitors *in vivo*.** **(A)**, Quantification of the number of DCX-
620 positive/GFP-positive LV-transduced cells in the SVZ, RMS and OB shows that the migration of
621 SEZ cells to the OB is not affected by post-mitotic induction of *Neurog2*. Error bars indicate
622 mean \pm s.d., $n=3/\text{group}$, n.s., non-significant, One-Way ANOVA followed by Tukey's HSD
623 post-hoc test. **(B)**, Micrograph showing neuroblasts (DCX, in red) leaving the SEZ and
624 expressing GFP (in green), indicative of lentiviral transduction with *Neurog2* and hSyn-promoter
625 activity in these cells. **(C,D)**, Micrographs of the granule layer of the OB showing lentivirally
626 transduced cells (green) migrating radially and integrating as granule and or periglomerular
627 neurons (PGN, insets, DCX red) at 10 DPI. **(E-F)**, SEZ cells transduction with the hSyn-*egfp*
628 control (green) and the hSyn-*Neurog2*-IRES-*egfp* (green) lentiviruses do not result in Tbr2
629 expression (red) in periglomerular (PGN, insets) or granule neurons. Scale bars: 50 μm
630 (B,C,D,E,F), 10 μm (insets in C,D,E,F).

631

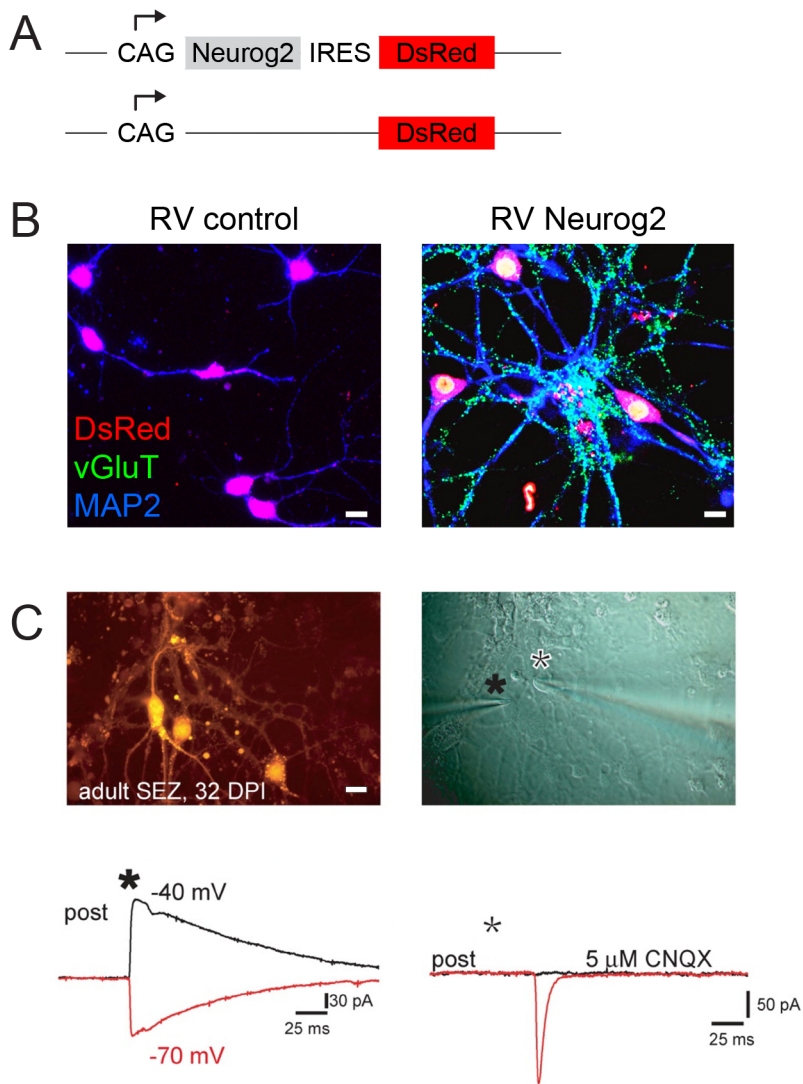


Figure 1

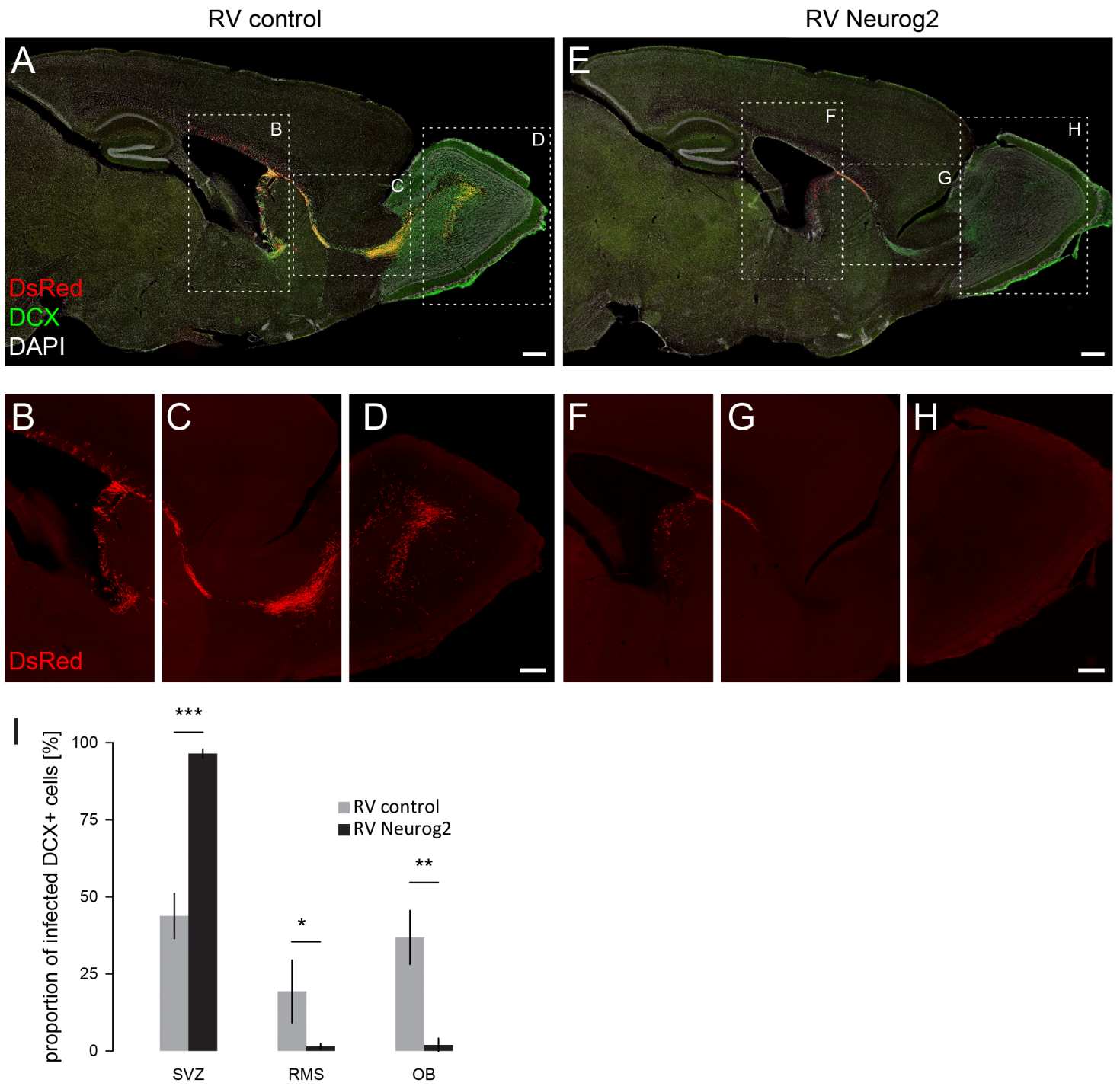


Figure 2

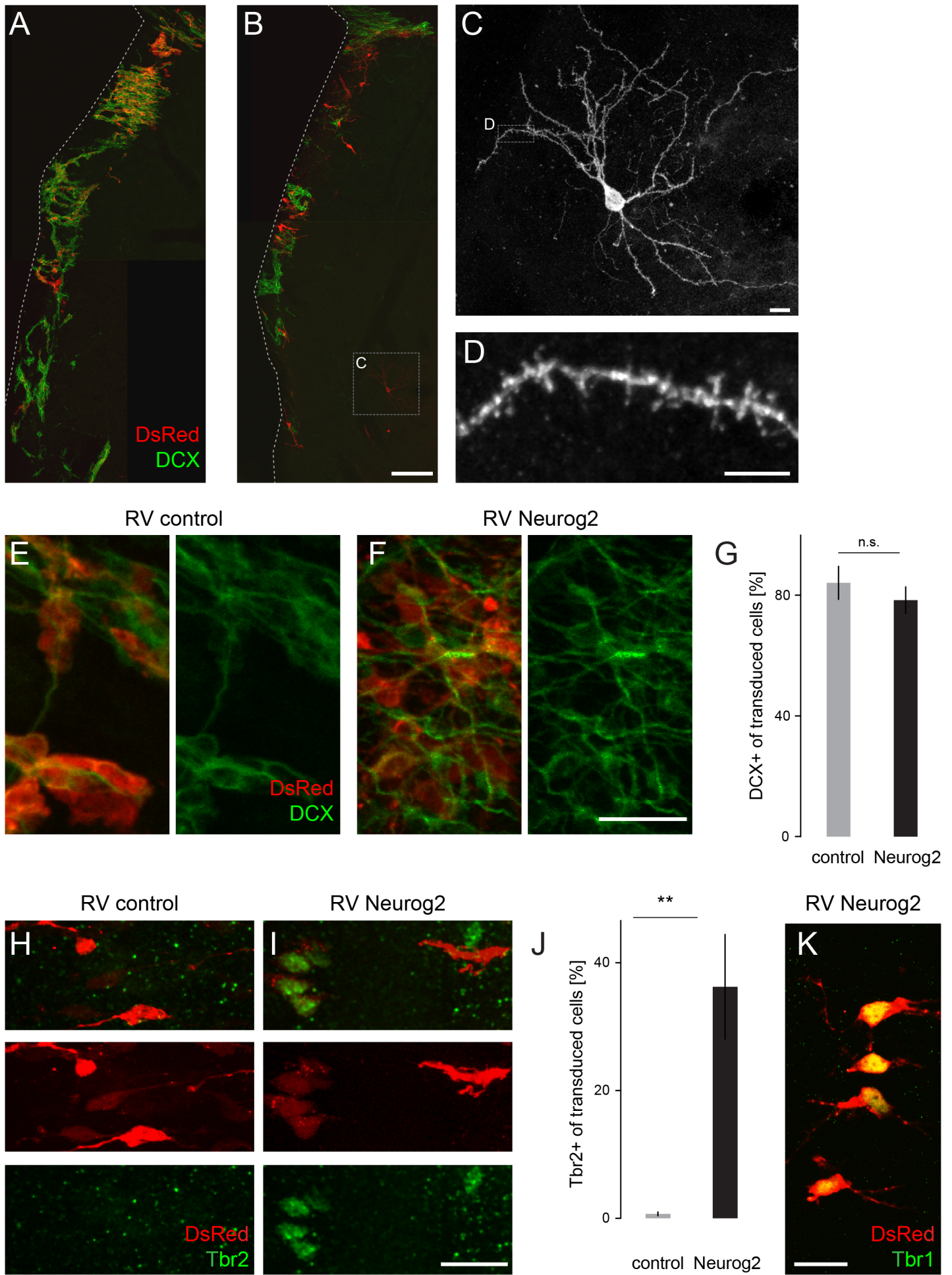


Figure 3

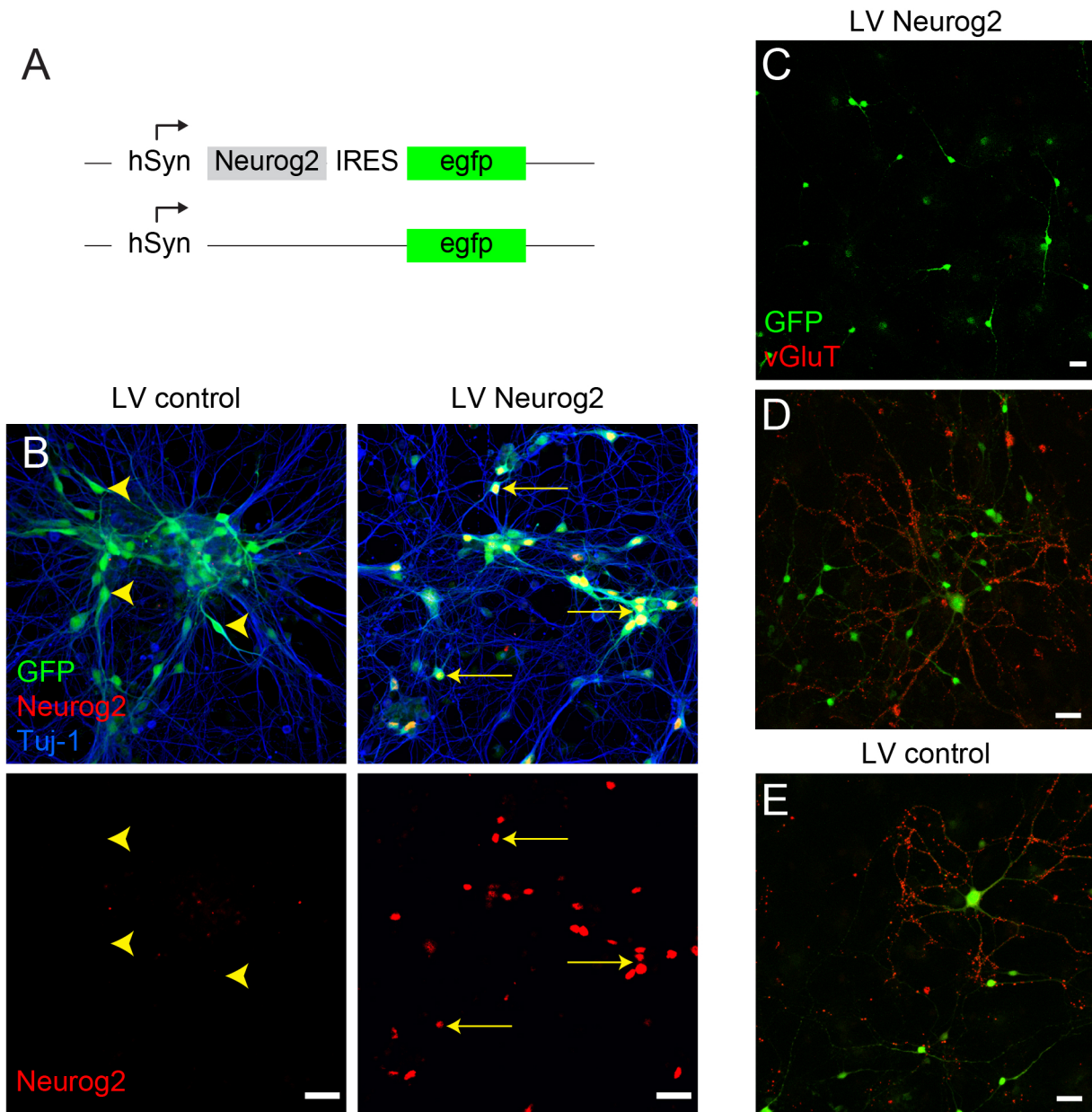


Figure 4

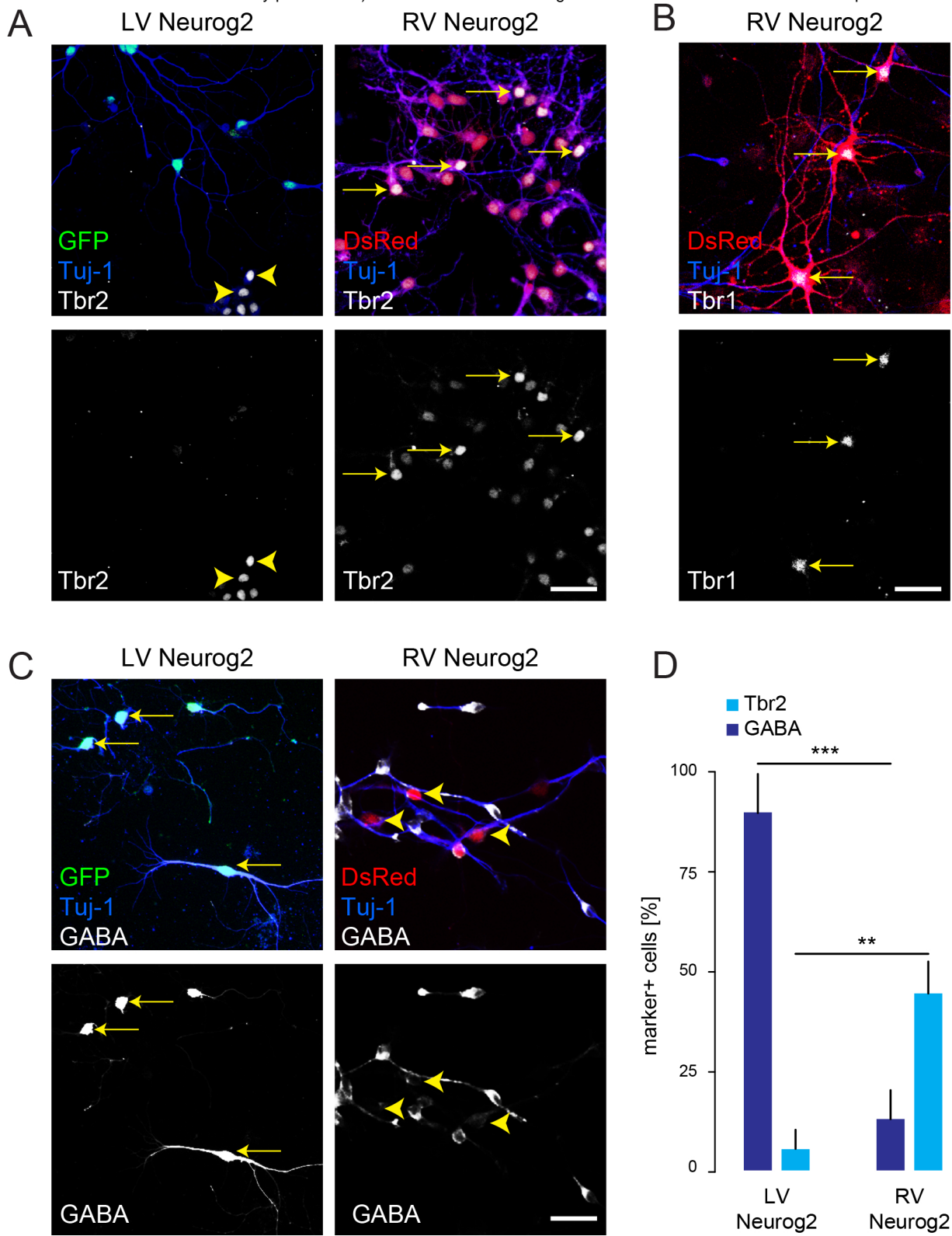


Figure 5

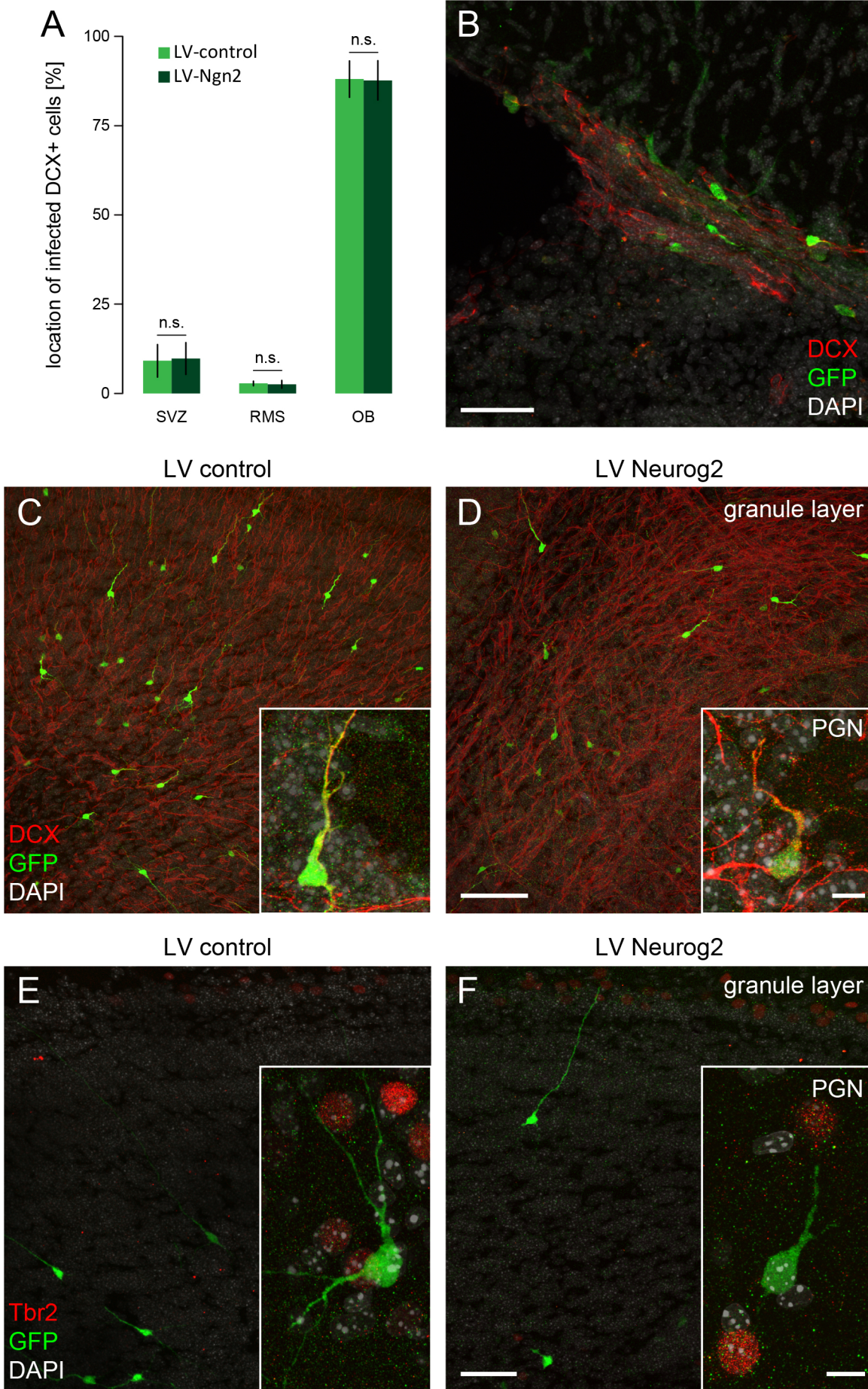


Figure 6